JOURNAL OF GUIDANCE, CONTROL, AND DYNAMICS
Vol. 22, No. 1, January–February 1999

New Design Method for Pulse-Width Modulation Control Systems via Digital Redesign

Tohru Ieko,* Yoshimasa Ochi,† and Kimio Kanai‡
National Defense Academy, Yokosuka 239-8686, Japan

A design method is proposed for pulse-width modulation (PWM) control systems, where magnitude of control input is fixed but pulse width is adjustable. In the proposed method, first a discrete-time (DT) control system of the amplitude modulation type is designed, and then it is converted into a PWM control system. Pulse width and delay time for PWM input are determined at each sampling time so that the state error between the DT and PWM control systems can be small. The DT controller is determined by digital redesign of a given continuous-time (CT) controller. The digital redesign method previously proposed by the authors is based on the principle of equivalent area. Thus, in spite of the inherent nonlinearity of PWM input, inasmuch as linear control theory can be employed in design of the baseline DT or CT controller, the PWM control system is obtained without using nonlinear control theory. In addition, because the proposed methods are described in state-space representation, they are applicable to multi-input/multi-output systems. The effectiveness of the methods is illustrated through computer simulation using a flexible spacecraft model.

Introduction

IN linear time-invariant (LTI) control systems, control is performed by modulating amplitude of the control input. On the other hand, systems with on/off type control inputs with fixed amplitude, such as reaction jets and electronic relays, are controlled by modulating not the amplitude but the firing pulse width of the control inputs. These systems are often called pulse-width modulation (PWM) control systems. Because of the nonlinearity of the PWM control inputs, PWM control systems have been analyzed and synthesized as nonlinear systems.[1,2] However, nonlinear methods, for example, the well-known describing function method, are generally complicated and inadequate to deal with multi-input/multi-output (MIMO) systems. This paper proposes a new design method for PWM control systems. In the proposed method, first a discrete-time (DT) LTI control system of the amplitude modulation type is designed, and then it is converted into a PWM control system. In the conversion, a pulse width and a delay time for PWM control input are determined at each sampling time so that the error between the DT and PWM states can be small. Because there are various established design methods for DT LTI control systems, we can choose an appropriate method in the DT controller design depending on control objective or specifications. In addition, once the DT controller is obtained, the pulse width and delay time are determined no matter what method is used in the DT controller design. Similar methodologies, based on the principle of equivalent area (PEA),[3] have been proposed in Refs. 4 and 5; however, our method is better in providing smaller error than Ref. 4. Although Ref. 5 modifies delay time τ in Ref. 4 as $\tau - W\sigma$, where σ is pulse width, W is not definitely given based on a clear mathematical discussion.

In this paper, we employ a digital redesign method for the DT controller design; that is, first a continuous time (CT) controller is designed and then it is converted into a DT controller. In the method used here, which was previously proposed by the authors,[6] the DT closed-loop control input is determined by the PEA so as to approximate the mean value of the CT closed-loop input during each sampling period. The resulting DT controller reproduces CT closed-loop state responses with good precision, as well as providing improved stability compared to open-loop redesign methods such as Tustin's method.[7]

The outline of this paper is as follows. The next section presents some background information on DT models and the PEA. The PWM control input formulation is shown in the section that follows, where it is shown that the obtained pulse width satisfies the PEA. Then a digital redesign method based on the PEA is presented. Next a design example for an attitude control system of a flexible artificial satellite is described with numerical simulation results. Finally, conclusions are given.

Preliminaries

Step Invariance DT Model

To express the relation between CT and DT systems better DT LTI systems are described in the delta operator form.[8] The operator is defined as $\varepsilon = (z - 1)/T = (e^{sT} - 1)/T$, where s, z, and T are the Laplace operator, the Z operator, and a sampling period, respectively. Obviously the relation $\lim_{T\to 0} \varepsilon = s$ holds. Because the delta and shift forms are theoretically equivalent, the content of this paper can be described using the shift operator. Consider a CT LTI system described by

$$\dot{\boldsymbol{x}}(t) = \boldsymbol{A}\boldsymbol{x}(t) + \boldsymbol{B}\boldsymbol{u}(t), \qquad \boldsymbol{A} \in R^{n\times n}, \qquad \boldsymbol{B} \in R^{n\times r} \tag{1}$$

$$\boldsymbol{y}(t) = \boldsymbol{C}\boldsymbol{x}(t) + \boldsymbol{D}\boldsymbol{u}(t), \qquad \boldsymbol{C} \in R^{p\times n}, \qquad \boldsymbol{D} \in R^{p\times r} \tag{2}$$

The solution of Eq. (1) is given by

$$\boldsymbol{x}(t_1) = \exp[\boldsymbol{A}(t_1 - t_0)]\boldsymbol{x}(t_0) + \int_{t_0}^{t_1} \exp[\boldsymbol{A}(t_1 - \rho)]\boldsymbol{B}\boldsymbol{u}(\rho)\,\mathrm{d}\rho \tag{3}$$

In Eq. (3), assuming that $t_0 = kT$, $t_1 = kT + T$ ($k = 0, 1, 2, \ldots$), and the input $\boldsymbol{u}$ is constant during each sampling interval, the step invariance model is defined as

$$\varepsilon\boldsymbol{x}(kT) = \frac{\boldsymbol{x}(kT + T) - \boldsymbol{x}(kT)}{T} = \boldsymbol{A}_S\boldsymbol{x}(kT) + \boldsymbol{B}_S\boldsymbol{u}(kT) \tag{4}$$

$$\boldsymbol{y}(kT) = C\boldsymbol{x}(kT) + \boldsymbol{D}\boldsymbol{u}(kT) \tag{5}$$

where

$$\boldsymbol{A}_S = \frac{e^{AT} - \boldsymbol{I}_n}{T}, \qquad \boldsymbol{B}_S = \int_0^T e^{A\rho}\frac{\mathrm{d}\rho\boldsymbol{B}}{T}$$

Received Dec. 8, 1997; revision received July 30, 1998; accepted for publication Aug. 17, 1998.

*Ph.D. Candidate, Department of Aerospace Engineering. Student Member AIAA.

†Associate Professor, Department of Aerospace Engineering. Member AIAA.

‡Professor, Department of Aerospace Engineering. Associate Fellow AIAA.

I_n is an $n \times n$ identity matrix. The state and output of this model are equal to those of the CT system at each sampling time. Furthermore, defining the function

$$E(A, T) = \sum_{n=0}^{\infty} \frac{(AT)^n}{(n+1)!}$$

A_s and B_s can be written as $A_s = E(A, T)A = AE(A, T)$ and $B_s = E(A, T)B$, respectively.

Step Average Model[6]

Assuming again that the input is constant during each sampling interval, a DT model whose output is the mean value of the CT system's output during each sampling interval can be derived as follows. This model is utilized in digital redesign based on the PEA.

Intersample output at $t = kT + m$ $(0 \le m \le T)$ is described by

$$y(kT+m) = Ce^{Am}x(kT) + \left(D + C\int_0^m e^{A\rho}\,d\rho\right)u(kT) \quad (6)$$

Then the mean value $\tilde{y}(kT)$ of the CT system's output for $kT \le t \le kT + T$ is obtained as

$$\begin{aligned}\tilde{y}(kT) &= \frac{1}{T}\int_0^T y(kT+m)\,dm \\ &= C\cdot E(A, T)x(kT) \\ &\quad + \left\{D + \frac{1}{T}C\int_0^T mE(A, m)\,dm B\right\}u(kT) \\ &:= \tilde{C}x(kT) + \tilde{D}u(kT)\end{aligned} \quad (7)$$

Note that the state equation of this model is the same as that of the step invariance model described by Eq. (4). Let us call the DT model defined by Eqs. (4) and (7) the step average model. Some characteristics of this DT model are as follows.

1) If both CT system and its step invariance model are minimal realization, then this model is also minimal realization.

2) Let us denote the poles of the CT system and the corresponding poles of the DT model as s and ε, respectively. Then they have the relation $\varepsilon = (e^{sT} - 1)/T$.

3) If the CT system is stable, then steady-state gains of the CT system and discrete model are equivalent, namely, $\tilde{D} - \tilde{C}A_S^{-1}B_S = D - CA^{-1}B$.

4) The matrices $\tilde{C}$ and $\tilde{D}$ can be calculated as

$$\begin{bmatrix} 0_{r\times r} & 0_{r\times p} & 0_{r\times n} \\ \tilde{D} & 0_{p\times p} & \tilde{C} \\ B_S & 0_{n\times p} & A_S \end{bmatrix} = \left(\exp\left\{\begin{bmatrix} 0_{r\times r} & 0_{r\times p} & 0_{r\times n} \\ D & 0_{p\times p} & C \\ B & 0_{n\times p} & A \end{bmatrix} T\right\} - I_{n+r+p}\right)\Bigg/ T \quad (8)$$

PEA

In this subsection we show that the PEA provides DT control input that reproduces time responses of the state to CT control input with a good precision. For $t_1 = t_0 + \Delta$ where $\Delta > 0$, Eq. (3) can be written as

$$x(t_0+\Delta) = e^{A\Delta}x(t_0) + \sum_{i=1}^{\infty} c_i \int_0^{\Delta} \rho^i u(t_0 + \Delta - \rho)\,d\rho \quad (9)$$

where $c_i = A^i B/i!$. Assuming constant input $u(t) = u_d(t_0)$ for $t_0 \le t \le t_0 + \Delta$, similarly to Eq. (4) we have

$$x_d(t_0+\Delta) = e^{A\Delta}x_d(t_0) + \sum_{i=1}^{\infty} c_i \int_0^{\Delta} \rho^i u_d(t_0)\,d\rho \quad (10)$$

From Eqs. (9) and (10), for the same initial state $x(t_0) = x_d(t_0)$, the state error between $x(t_0+\Delta)$ and $x_d(t_0+\Delta)$ is obtained as

$$x(t_0+\Delta) - x_d(t_0+\Delta) = \sum_{i=0}^{\infty} c_i \int_0^{\Delta} \rho^i U(\rho)\,d\rho \quad (11)$$

where $U(\rho) = u(t_0 + \Delta - \rho) - u_d(t_0)$. To make the first term in Eq. (11) zero, we require

$$u_d(t_0) = \frac{1}{\Delta}\int_{t_0}^{t_0+\Delta} u(\rho)\,d\rho \quad (12)$$

Equation (12) implies the PEA. By applying the integral mean value theorem to the terms higher than the second in ρ, there exists $h_i \in [0, \Delta]$ that satisfies

$$\int_0^{\Delta} \rho^i U(\rho)\,d\rho = U(h_i)\int_0^{\Delta}\rho^i\,d\rho = U(h_i)\frac{\Delta^{i+1}}{i+1} \quad (13)$$

With Eqs. (12) and (13), the state error becomes

$$x(t_0+\Delta) - x_d(t_0+\Delta) = \sum_{i=1}^{\infty} c_i U(h_i)\frac{\Delta^{i+1}}{i+1} \quad (14)$$

Thus, the constant input $u_d(t_0)$ given by Eq. (12) makes the error between the CT and DT states at $t = t_0 + \Delta$ of order Δ^2; hence, the DT input reproduces the CT state precisely for a small Δ.

PWM Control Law

Consider the input shown in Fig. 1, where fixed magnitude, pulse width, and delay time are $\bar{u}_p, \sigma(kT)$, and $\tau(kT)$, respectively. In MIMO systems, similarly we define $\bar{u} = [\bar{u}_1\ \bar{u}_2\ \cdots\ \bar{u}_r]^T$, $\sigma(kT) = \mathrm{diag}\{\sigma_i(kT)\}$, and $\tau(kT) = \mathrm{diag}\{\tau_i(kT)\}$ $(i = 1, \ldots, r)$, where diag{ } is a diagonal matrix with diagonal elements { } and the ith element of $\bar{u}$ takes $\bar{u}_i = -\bar{u}_{pi}$, 0, or $\bar{u}_{pi}$. Given a state vector $x(kT)$, the state at $t = kT + T$ for the PWM control input is described as

$$\bar{x}(kT+T) = e^{AT}x(kT) + \sum_{i=1}^{r}\left\{\exp[A(T - \tau_i - \sigma_i)]\int_0^{\sigma_i} e^{A\rho}\,d\rho\, b_i \bar{u}_i\right\} \quad (15)$$

where b_i is the ith column of B. From Eqs. (4) and (15) we obtain the error between the states at $t = kT + T$ as

$$\begin{aligned} x(kT+T) - \bar{x}(kT+T) &= E(A, T)TBu(kT) \\ &\quad - \sum_{i=1}^{r} \exp\{A[T - \tau_i(kT) - \sigma_i(kT)]\}E\{A, \sigma_i(kT)\}\sigma_i(kT)b_i\bar{u}_i \\ &:= R(T^1) + R(T^2) + R(T^3) + \cdots \end{aligned} \quad (16)$$

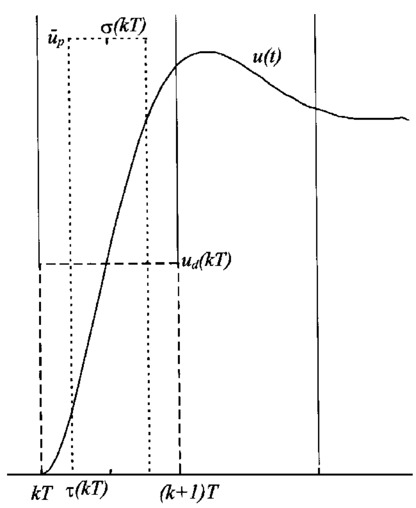

Fig. 1 Equivalent areas for CT, DT, and PWM control inputs.

where

$$R(T^1) = \boldsymbol{B}\{T\boldsymbol{u}(kT) - \boldsymbol{\sigma}(kT)\bar{\boldsymbol{u}}\} \tag{17}$$

$$R(T^2) = \boldsymbol{AB}\left[\frac{T}{2}\{T\boldsymbol{u}(kT) - \boldsymbol{\sigma}(kT)\bar{\boldsymbol{u}}\} + \frac{-T\boldsymbol{I}_r + 2\boldsymbol{\tau}(kT) + \boldsymbol{\sigma}(kT)}{2}\boldsymbol{\sigma}(kT)\bar{\boldsymbol{u}}\right] \tag{18}$$

Then to make $R(T^1)$ and $R(T^2)$ zero for the jth ($j = 1, 2, \ldots, r$) control input, select its amplitude, pulse width, and delay time as

$$\bar{u}_j = \mathrm{sign}\{u_j(kT)\} \cdot \bar{u}_{pj} \tag{19}$$

$$\sigma_j(kT) = \frac{Tu_j(kT)}{\bar{u}_j} \tag{20}$$

$$\tau_j(kT) = \frac{\{T - \sigma_j(kT)\}}{2} \tag{21}$$

respectively. With Eqs. (20) and (21) the resulting third-order term in T in Eq. (16) becomes $R(T^3) = \boldsymbol{A}^2\boldsymbol{B}T\{T^2\boldsymbol{I}_r - \sigma^2(kT)\}\boldsymbol{u}(kT)/24$. Note that Eq. (20) implies the PEA and that the delay time given by Eq. (21) means that the center of the pulse width should be $(k + 1/2)T$, i.e., the center of the sampling period. This delay time is different from the results shown in Refs. 4 and 5, which consider the first-order term only.

Because a practical PWM control system has a minimum pulse width $\sigma_{\min}$, a required pulse width may not be realized exactly. Particularly, as shown in a design example later, control performance depends on $N = T/\sigma_{\min}$, that is, the larger N, the smaller the state error. In this paper we assume that N is large enough to guarantee a small state error.

Digital Redesign Based on PEA

In open-loop digital redesign methods, such as Tustin's, a very small sampling period is often required to guarantee stability and a good control performance. To ensure a larger N, closed-loop digital redesign methods that allow a larger sampling period are desirable. In this section, a closed-loop digital redesign method, which was initially presented in Ref. 6, is represented. In what follows we consider redesigning a CT unity-feedback control system shown in Fig. 2a as a DT one in Fig. 2b. In Fig. 2, $\boldsymbol{P}(s)$, $\boldsymbol{K}(s)$, $\boldsymbol{K}_d(\varepsilon)$, $\boldsymbol{u}(t)$, and $\boldsymbol{u}_d(kT)$ are the CT plant model, the CT controller, redesigned DT controller, and the CT and DT control inputs, respectively, and the broken lines indicate DT signal flow. Given $\boldsymbol{K}(s)$, our goal is to determine $\boldsymbol{K}_d(\varepsilon)$ that duplicates state responses of the CT control system.

Equation (14) suggests that the DT control input

$$\boldsymbol{u}_d(kT) = \frac{1}{T}\int_{kT}^{kT+T} \boldsymbol{u}(\rho)\,\mathrm{d}\rho \tag{22}$$

make the state error between the CT and DT systems small. Figure 1 shows $u(t)$ and $u_d(kT)$ in a scalar case. To match closed-loop time responses of the states, we consider closed-loop CT control input; in other words, we consider a closed-loop transfer function from the external input $\boldsymbol{w}(t)$ to the plant input $\boldsymbol{u}(t)$. Let us call the transfer function the plant input transfer function (PITF). Note that given a CT PITF, its step average model provides $\boldsymbol{u}_d(kT)$ in Eq. (22). The preceding observation leads to a three-step redesigning procedure.

1) Calculate a CT PITF for the CT control system.
2) By discretizing the CT PITF as a step average model, obtain a DT PITF that generates DT input of Eq. (22).
3) Find $\boldsymbol{K}_d(\varepsilon)$ from the DT PITF.

This redesign methodology of discretizing the CT PITF was originally proposed in Ref. 9. However, our method is new in discretizing as a step average model and in the method of finding the DT controller, which makes the method applicable to MIMO systems as well.

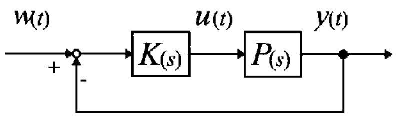

Fig. 2a CT control system.

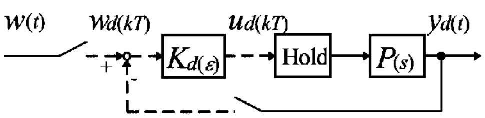

Fig. 2b DT control system.

In the following we describe the redesign method more in detail. In Fig. 2a, let state-space representations of the CT plant and controller be

$$\boldsymbol{P}(s) := \left[\begin{array}{c|c}\boldsymbol{A}_P & \boldsymbol{B}_P \\ \hline \boldsymbol{C}_P & \boldsymbol{D}_P\end{array}\right], \qquad \boldsymbol{K}(s) := \left[\begin{array}{c|c}\boldsymbol{A}_K & \boldsymbol{B}_K \\ \hline \boldsymbol{C}_K & \boldsymbol{D}_K\end{array}\right]$$

respectively. Then the CT PITF is obtained as

$$\boldsymbol{H}(s) := \left[\begin{array}{c|c}\boldsymbol{A}_H & \boldsymbol{B}_H \\ \hline \boldsymbol{C}_H & \boldsymbol{D}_H\end{array}\right] := \left[\begin{array}{cc|c}\boldsymbol{A}_{H11} & \boldsymbol{A}_{H12} & \boldsymbol{B}_{H1} \\ \boldsymbol{A}_{H21} & \boldsymbol{A}_{H22} & \boldsymbol{B}_{H2} \\ \hline \boldsymbol{C}_{H1} & \boldsymbol{C}_{H2} & \boldsymbol{D}_H\end{array}\right] \tag{23}$$

where

$$\boldsymbol{A}_H = \left[\begin{array}{c:c}\boldsymbol{A}_P - \boldsymbol{B}_P\boldsymbol{D}_0^{-1}\boldsymbol{D}_K\boldsymbol{C}_P & \boldsymbol{B}_P\boldsymbol{D}_0^{-1}\boldsymbol{C}_K \\ \hdashline \boldsymbol{B}_K\left(\boldsymbol{D}_P\boldsymbol{D}_0^{-1}\boldsymbol{D}_k - \boldsymbol{I}\right)\boldsymbol{C}_P & \boldsymbol{A}_K - \boldsymbol{B}_K\boldsymbol{D}_P\boldsymbol{D}_0^{-1}\boldsymbol{C}_K\end{array}\right]$$

$$\boldsymbol{B}_H = \left[\begin{array}{c}\boldsymbol{B}_P\boldsymbol{D}_0^{-1}\boldsymbol{D}_K \\ \hdashline \boldsymbol{B}_K\left(\boldsymbol{I} - \boldsymbol{D}_P\boldsymbol{D}_0^{-1}\boldsymbol{D}_K\right)\end{array}\right]$$

$$\boldsymbol{C}_H = \left[\begin{array}{c:c}-\boldsymbol{D}_0^{-1}\boldsymbol{D}_K\boldsymbol{C}_P & \boldsymbol{D}_0^{-1}\boldsymbol{C}_K\end{array}\right]$$

$$\boldsymbol{D}_H = \boldsymbol{D}_0^{-1}\boldsymbol{D}_K \qquad \boldsymbol{D}_0 = \boldsymbol{I} + \boldsymbol{D}_K\boldsymbol{D}_P$$

The DT step average model of $\boldsymbol{H}(s)$ is obtained as

$$\tilde{\boldsymbol{H}}_d(\varepsilon) = \left[\begin{array}{c|c}\boldsymbol{A}_{HS} & \boldsymbol{B}_{HS} \\ \hline \tilde{\boldsymbol{C}}_H & \tilde{\boldsymbol{D}}_H\end{array}\right] = \left[\begin{array}{cc|c}\boldsymbol{A}_{HS11} & \boldsymbol{A}_{HS12} & \boldsymbol{B}_{HS1} \\ \boldsymbol{A}_{HS21} & \boldsymbol{A}_{HS22} & \boldsymbol{B}_{HS2} \\ \hline \tilde{\boldsymbol{C}}_{H1} & \tilde{\boldsymbol{C}}_{H2} & \tilde{\boldsymbol{D}}_H\end{array}\right] \tag{24}$$

where $\boldsymbol{A}_{HS}$, $\boldsymbol{B}_{HS}$, $\tilde{\boldsymbol{C}}_H$, and $\tilde{\boldsymbol{D}}_H$ can be calculated by Eq. (8).

In the CT closed-loop transfer function $\boldsymbol{P}(s)\boldsymbol{H}(s)$, because the poles of the plant are canceled by some zeros of $\boldsymbol{H}(s)$, the closed-loop poles of $\boldsymbol{P}(s)\boldsymbol{H}(s)$ are the same as the poles of $\boldsymbol{H}(s)$. On the other hand, in the DT closed-loop transfer function $\boldsymbol{P}_S(\varepsilon)\tilde{\boldsymbol{H}}_d(\varepsilon)$, this cancellation does not occur, where $\boldsymbol{P}_s(\varepsilon)$ is a step invariance model of the CT plant. Thereby, the order of the DT controller obtained from $\tilde{\boldsymbol{H}}_d(\varepsilon)$ increases by the order of the plant as compared to that obtained from a DT PITF, which has the plant poles as its zeros.

To settle this problem we modify the DT PITF as

$$\boldsymbol{H}_d(\varepsilon) := \left[\begin{array}{cc|c}\boldsymbol{A}_S + \boldsymbol{B}_S\tilde{\boldsymbol{C}}_{H1} & \boldsymbol{B}_S\tilde{\boldsymbol{C}}_{H2} & \boldsymbol{B}_S\tilde{\boldsymbol{D}}_H \\ A_{HS21} & A_{HS22} & B_{HS2} \\ \hline \boldsymbol{C}_{H1} & \tilde{\boldsymbol{C}}_{H2} & \tilde{\boldsymbol{D}}_H\end{array}\right] \tag{25}$$

where $A_S = E(A_P, T)A_P$ and $B_S = E(A_P, T)B_P$. Note that the DT closed-loop state equation for the plant is similar to that of the CT counterpart; that is, compare the DT equation

$$\varepsilon x_p = A_S x_p + B_S[\tilde{C}_{H1} \quad \tilde{C}_{H2} \quad \tilde{D}_{H2}]\begin{bmatrix} x_p^T & x_c^T & w^T \end{bmatrix}^T$$

to the CT equation

$$\dot{x}_p = A_P x_p + B_P[C_H \mid D_H]\begin{bmatrix} x_p^T & x_c^T \mid w^T \end{bmatrix}^T$$

Then, as in the CT case, we have

$$P_S(\varepsilon)H_d(\varepsilon) = \left[\begin{array}{c:c|c} A_S + B_S\tilde{C}_{H1} & B_S\tilde{C}_{H2} & B_S\tilde{D}_H \\ \hdashline A_{HS21} & A_{HS22} & B_{HS2} \\ \hline C_P + D_P\tilde{C}_{H1} & D_P\tilde{C}_{H2} & D_P\tilde{D}_H \end{array}\right] \tag{26}$$

which indicates that the plant poles are canceled by some zeros of $H_d(\varepsilon)$. However, the closed-loop poles of the modified DT PITF $H_d(\varepsilon)$ become different from those of $\tilde{H}_d(\varepsilon)$, which are given by eigenvalues of A_{HS}; therefore, the poles of $H_d(\varepsilon)$ are not related to those of $H(s)$ by $\varepsilon = (e^{sT} - 1)/T$. Because closed-loop characteristics should be maintained through redesign, we need to compare the state matrix of $\tilde{H}_d(\varepsilon)$ or A_{HS} to that of $H_d(\varepsilon)$. By applying the Taylor series expansion to the exponential functions in the submatrices in Eq. (26) and using the first-order approximation (FOA), we have

$$\begin{aligned} A_S + B_S\tilde{C}_{H1} &\approx \left(A_P - B_P D_0^{-1} D_K C_P\right) \\ &\quad + \left(A_P - B_P D_0^{-1} D_K C_P\right)^2 T/2 \\ &\quad + B_P D_0^{-1} C_K B_K \left(D_P D_0^{-1} D_K - I\right) C_K T/2 \\ &= A_{H11} + A_{H11}^2 T/2 + A_{H12} A_{H21} T/2 \end{aligned} \tag{27}$$

$$\begin{aligned} B_S\tilde{C}_{H2} &\approx B_P D_0^{-1} C_K + \left(A_P - B_P D_0^{-1} D_K C_P\right) B_P D_0^{-1} C_K T/2 \\ &\quad + B_P D_0^{-1} C_K \left(A_K - B_K D_P D_0^{-1} C_K\right) T/2 \\ &= A_{H12} + A_{H11} A_{H12} T/2 + A_{H12} A_{H22} T/2 \end{aligned} \tag{28}$$

where the following FOAs are used:

$$\begin{aligned} \lfloor \tilde{C}_{H1} \quad \tilde{C}_{H2} \rfloor &= [C_{H1} \quad C_{H2}] E(A_H, T) \\ &\approx [C_{H1} \quad C_{H2}](I + A_H T/2) \\ A_S = E(A_P, T)A_P &\approx A_P + A_P^2 T/2 \\ B_S = E(A_P, T)B_P &\approx B_P + A_P B_P T/2 \end{aligned}$$

Equations (27) and (28) show that in terms of the FOA the submatrices agree with A_{HS11} and A_{HS12}, respectively. This indicates that the state matrix of $H_d(\varepsilon)$ agrees with A_{HS}, the state matrix of $\tilde{H}_d(\varepsilon)$, at least in the FOA. Therefore, the closed-loop poles of $H_d(\varepsilon)$ are close to those of $\tilde{H}_d(\varepsilon)$ for small sampling periods, which means the CT poles are approximately related to DT poles by $\varepsilon = (e^{sT} - 1)/T$. Likewise, we obtain the FOA,

$$\begin{aligned} B_S\tilde{D}_H &\approx B_P D_H + (B_P C_H B_H + A_P B_P D_H)T/2 \\ &= (I + A_{H11}T/2)B_{H1} + A_{H12} B_{H2} T/2 \end{aligned} \tag{29}$$

The right-hand side is also the FOA of B_{HS1} in Eq. (24). Thus, the state-space representation of $H_d(\varepsilon)$ agrees with that of $\tilde{H}_d(\varepsilon)$, at least in the FOA; as a result, the closed-loop characteristics such as stability are preserved, unless T is too large.

It can also be shown that the CT and redesigned DT control systems have the same steady-state gain, when the DT control system is stable.[6]

To find a DT controller $K_d(\varepsilon)$ that realizes the DT PITF $H_d(\varepsilon)$, we take an approach based on H_∞ control. Namely, we consider finding a stabilizing DT controller satisfying

$$\left\| -H_d(\varepsilon) + K_d(\varepsilon)\{I + P_S(\varepsilon)K_d(\varepsilon)\}^{-1} \right\|_\infty \le \gamma \tag{30}$$

where γ is a positive number to be minimized through iteration. Note that the second term in the cost function is the DT PITF for a DT controller $K_d(\varepsilon)$; hence, this is a kind of model matching problem. For stable plants, $\gamma = 0$, i.e., exact model matching is always achieved.[10] In fact, the DT controller can also be obtained by solving Eq. (29) for $\gamma = 0$ for $K_d(\varepsilon)$. However, a simple calculation reveals that pole-zero cancellation with respect to plant poles occurs to the resulting DT PITF. This means that if the poles include an unstable one the closed-loop system becomes unstable. In such a case, H_∞ control yields a stabilizing controller at the cost of exact model matching, where γ cannot be made zero. In practice we are often required to achieve model matching in some specified frequency ranges. Hence, for unstable plants we modify the cost function as

$$\left\| W_a(\varepsilon)\left[-H_d(\varepsilon) + K_d(\varepsilon)\{I + P_S(\varepsilon)K_d(\varepsilon)\}^{-1}\right] \right\|_\infty < \gamma \tag{31}$$

where $W_a(\varepsilon)$ is a weighting function that has large gains in appropriate frequency ranges. The DT H_∞ control problem in delta form can be solved by using the CT algorithm via the bilinear transform in the same way as in the shift form.

In the case of state feedback, a digital redesign method based on the same methodology is shown in Ref. 11 with an aerospace application.

Design Example

In this section, the proposed method is applied to design of a yaw angle PWM control system for a flexible spacecraft shown in Ref. 1. We consider a one-degree-of-freedom motion about the yaw axis. The plant model including three flexible modes is given by

$$P(s) = 57.3\prod_{i=1}^{3}\left(\frac{s^2}{z_i^2} + \frac{2\zeta s}{z_i} + 1\right) \Bigg/ Js^2\prod_{i=1}^{3}\left(\frac{s^2}{p_i^2} + \frac{2\zeta s}{p_i} + 1\right) \tag{32}$$

where $z_1 = 1.0$, $z_2 = 2.0$, $z_3 = 7.2$, $p_1 = 1.1$, $p_2 = 3.5$, $p_3 = 7.3$, $\zeta = 0.002$, and $J = 2150$ kgm^2. In this plant model, the input is a torque of $\bar{u}_P = 2$ Nm produced by a pair of thrusters, and the output is yaw angle (deg). In controller design, we use the following simplified model:

$$P_{\text{design}}(s) = \left[\begin{array}{cc|c} 0 & 0 & 1 \\ 1 & 0 & 0 \\ \hline 0 & 57.3/J & 0 \end{array}\right] \tag{33}$$

First we design a CT linear state feedback control system with an observer, and then convert it into a unity-feedback CT control system. The state feedback gain and observer gain matrices are determined by the pole assignment technique for specified closed-loop poles of $-0.2 \pm 0.15j$. The resulting CT controller is

$$K(s) = \left[\begin{array}{cc|c} -0.4 & -0.125 & -2.3451 \\ 1 & -0.4 & -15.009 \\ \hline -0.4 & -0.0625 & 0 \end{array}\right] \tag{34}$$

By the proposed digital redesign method, a DT controller for $T = 1$ s is obtained as

$$K_d(\varepsilon) = \frac{0.7340(\varepsilon + 1.786)(\varepsilon + 0.07510)(\varepsilon + 0.01)^2}{(\varepsilon + 0.0045)(\varepsilon + 0.0203)(\varepsilon^2 + 0.75\varepsilon + 0.206)} \tag{35}$$

where the plant model $P_S(s) = P_{\text{design}}(s)$ used in Eq. (30) is modified to be $57.3/J(s + 0.01)^2$. Otherwise pole-zero cancellation occurs at $s = 0$ or $\varepsilon = 0$.

Figure 3 shows a PWM control system for the spacecraft. In computer simulation, yaw angle command is chosen to be a step of 1.5 deg, and it is assumed that the minimum pulse width is 0.01 s. In Fig. 3 the dashed lines indicate DT signals, and the sensor dynamics[1] is given by

$$G_{\text{sen}}(s) = \frac{1}{0.025^2 s^2/12 + 0.025s/2 + 1} \tag{36}$$

Although the sensor dynamics and a computation time delay of 0.1 s are not taken into account in controller design, they are considered in simulation.

The proposed PWM control method is compared with the method in Ref. 4. Figure 4a shows time histories of yaw angle for a sampling period of $T = 1$ s. The same DT controller $K_d(\varepsilon)$ is used in both PWM control methods. Whereas the output response by the method in Ref. 4 does not follow the CT response, the proposed method achieves good agreement with the CT output. Note that performance of the PWM control should be evaluated by the error between the CT and DT outputs. Both PWM control inputs for $0 \le t \le 6$ s are shown in Fig. 4b, where the solid lines and dashed lines indicate CT and PWM control inputs, respectively. In this example, as Fig. 4 shows, the pulse delay given by Ref. 4 becomes $T/2$; as a result, the available pulse width becomes smaller than $T/2$ because in Ref. 4 the pulse width is also determined by the PEA. Hence, when the absolute value of the DT input signal is larger than $\bar{u}_p/2$, the pulse width greater than $T/2$ is required, but this cannot be realized due to saturation of pulse width. For this reason, the method in Ref. 4 cannot precisely reproduce the output of the redesigned DT control system. By contrast, in the proposed method, because the center of pulse width is always in the middle of the sampling period, the pulse width is not saturated unless the absolute value of the DT control input is larger than $\bar{u}_p$. This results in a more precise agreement with the CT output.

Next, the digital redesign method based on the PEA is evaluated by comparing to Tustin's method, which is widely used in industry. In either case, the proposed PWM control method is used in conversion of the DT input to the PWM input. Figure 5 shows time histories of yaw angle for $T = 1$ s. From the result we can see that the redesigning capability of the proposed method is superior to Tustin's method in duplicating the CT output. Figures 6a and 6b show time histories for $T = 4$ s. Whereas the proposed method still produces the output close to the CT output for such a large sampling period, the performance of Tustin's method deteriorates.

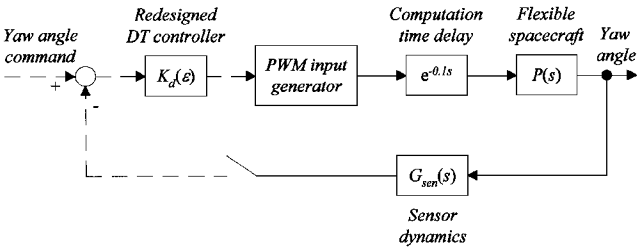

Fig. 3 PWM control system for a spacecraft.

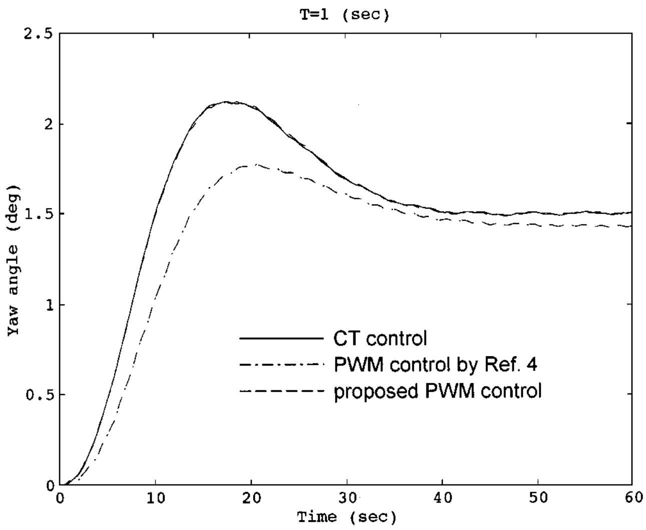

Fig. 4a Time histories of yaw angle, *T* = 1.0 s.

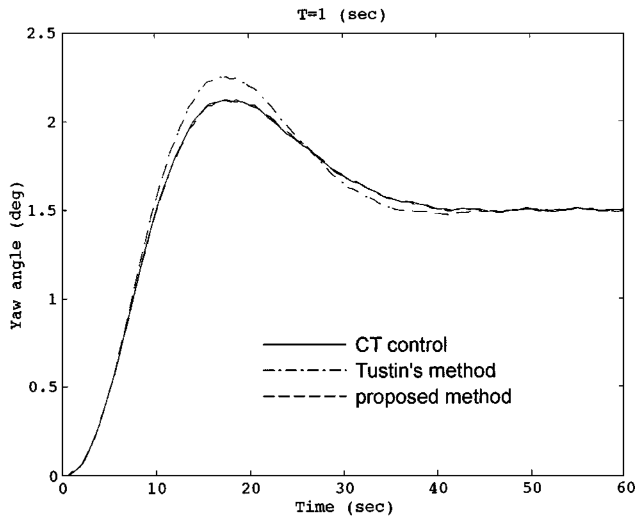

Fig. 5 Time histories of yaw angle, *T* = 1.0 s.

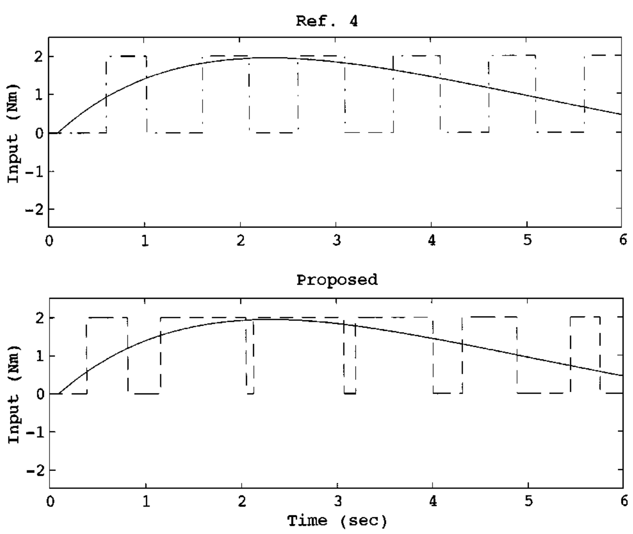

Fig. 4b Time histories of PWM input, *T* = 1.0 s.

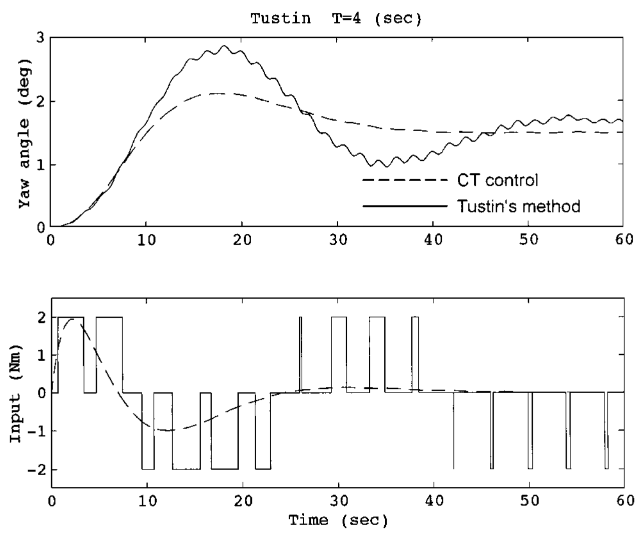

Fig. 6a Time histories of Tustin's method, *T* = 4 s.

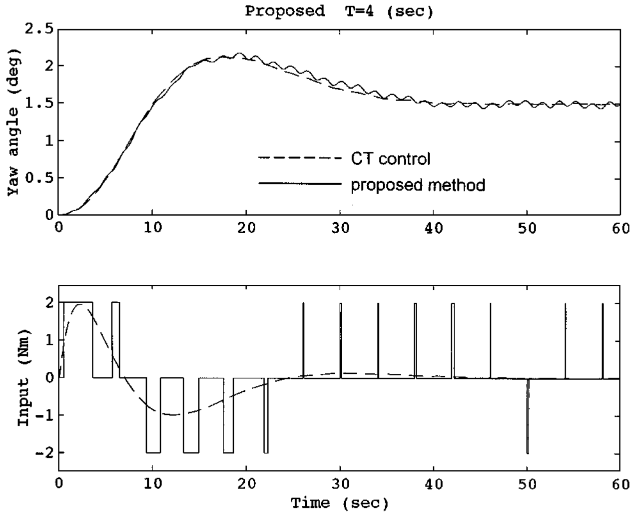

Fig. 6b Time histories of proposed method, *T* = 4 s.

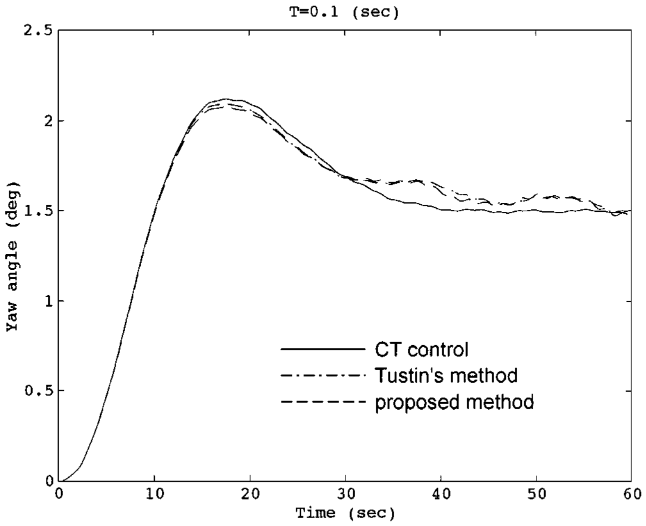

Fig. 7 Time histories of yaw angle, *T* = 0.1.

To see the effect of the maximum number of pulses in a sampling period, $N = T/\sigma_{\min}$, computer simulation was conducted for a smaller sampling period of $T = 0.1$ s. Although smaller sampling periods are generally favorable for digital redesign, the output responses, as shown in Fig. 7, are not improved, rather they are worse, as compared to the case of $T = 1$ s. This can be attributed to the error between the desired pulse width $\sigma(kT)$ and the realizable one $i(kT)\sigma_{\min}$, where $i(kT)$ is an integer for which $i(kT)\sigma_{\min}$ best approximates $\sigma(kT)$. In this example, because the sampling period $T = 0.1$ s is relatively small as compared to the minimum pulse width $\sigma_{\min} = 0.01$ s, the realizable pulse width cannot be a close approximation. However, this $\sigma_{\min}$ is much larger than values used in actual spacecraft; therefore, in practice a better approximation is achieved for such a short sampling period.

Conclusions

A new design method for PWM control systems is proposed. The methodology consists of three steps: 1) design of a CT control system, 2) redesign of the CT controller into a DT one, and 3) determining a pulse width and a delay time of PWM control input from DT control input. The pulse width and delay time, which are independent of plant parameters, are determined so that the state error between the DT and PWM control systems can be small. The result shows that the pulse width satisfies the PEA. For digital redesign in the second step, a new redesign method is proposed. The DT controller is derived by applying the PEA to discretization of a closed-loop plant input transfer function and using an H_∞ model matching technique. These methods are applied to design of a PWM attitude control system for a flexible spacecraft, and through computer simulation it is shown that the method provides control performance better than previously proposed methods.

References

[1]Anthony, T. C., and Wie, B., "Pulse-Modulated Control Synthesis for Flexible Spacecraft," *Journal of Guidance, Control, and Dynamics*, Vol. 13, No. 6, 1990, pp. 1014–1022.

[2]Shigehara, M., *Introduction to Space Engineering—Navigation and Control of Artificial Satellite and Rocket*, Baifuukan, Tokyo, 1994, pp. 49–60 (in Japanese).

[3]Andeen, R. E., "The Principle of Equivalent Area," *Proceedings of the AIEE Pacific General Meeting* (San Diego, CA), Vol. 79, American Inst. of Electrical Engineers, Applications and Industry, 1960, pp. 332–336.

[4]Bernelli-Zazzera, F., and Mantegazza, P., "Pulse-Width Equivalent to Pulse-Amplitude Discrete Control of Linear Systems," *Journal of Guidance, Control, and Dynamics*, Vol. 15, No. 2, 1992, pp. 461–467.

[5]Zimpfer, D. J., Shieh, L. S., and Sunkel, J. W., "Digitally Redesigned Pulse-Width Modulation Spacecraft Control," *Journal of Guidance, Control, and Dynamics*, Vol. 21, No. 4, 1998, pp. 529–534.

[6]Ieko, T., Ochi, Y., Kanai, K., and Hori, N., "Digital Redesign Methods Based on Plant Input Mapping and a New Discrete-Time Model," *Proceedings of 35th IEEE Conference on Decision and Control* (Kobe, Japan), Inst. of Electrical and Electronics Engineers, New York, 1996, pp. 1569–1574.

[7]Franklin, G. F., Powell, J. D., and Workman, M. L., *Digital Control of Dynamic Systems*, Addison–Wesley, Reading, MA, 1990, pp. 135–147.

[8]Middleton, R. H., and Goodwin, G. C., *Digital Control and Estimation—A Unified Approach*, Prentice–Hall, Englewood Cliffs, NJ, 1990, pp. 27–53.

[9]Markazi, A. H. D., and Hori, N., "A New Method with Guaranteed Stability for Discretization of Continuous-Time Control Systems," *Proceedings of 1992 American Control Conference* (Chicago, IL), Omnipress, Madison, WI, Vol. 2, 1992, pp. 1397–1402.

[10]Doyle, J. C., Glover, K., Khargoneker, P., and Francis, B., "State-Space Solutions to H_2 and H_∞ Control Problems," *IEEE Transactions on Automatic Control*, Vol. 34, No. 8, 1989, pp. 831–847.

[11]Ieko, T., Ochi, Y., and Kanai, K., "A New Digital Redesign Method for Pulse-Width Modulation Control Systems," *Proceedings of the AIAA Guidance, Navigation, and Control Conference* (New Orleans, LA), AIAA, Reston, VA, 1997, pp. 1730–1737.